Effect of Electric Field on the Degradation Process of Reinforced Mortar under Chloride and Sulfate Attack

Xiaotong Yu[1], Shagang Li[1], Xidong Chang[1], Yingdi Liao[1] and Da Chen[1]

[1]College of Harbor, Coastal, and Offshore Engineering, Hohai University, Nanjing 210098, PR China,
xiaotongyu@hhu.edu.cn (Xiaotong Yu), lishagang@hhu.edu.cn (Shagang Li),
changxidong@hhu.edu.cn (Xidong Chang), liaoyingdi@hhu.edu.cn (Yingdi Liao),
chenda@hhu.edu.cn (Da Chen, Corresponding author)

Abstract. *This study investigated the degradation mechanism behind the reinforced mortar exposed to chloride, sulfate and electric field. The steel-mortar samples were exposed to 5% Na_2SO_4, 5% NaCl + 5% Na_2SO_4 solutions and deionized water in two regimes (full immersion and direct current electric field). The efficiencies of three current densities were compared as well. The total and free sulfate ion content in the mortar were measured. The microstructural analysis by scanning electron microscopy (SEM), and energy dispersive X-ray spectroscopy (EDS) were conducted. The results indicated that the electric field drastically increased the ingress of sulfate, as well as the sulfate reaction. Meanwhile, the current attenuated the interaction between chloride and sulfate. The increase in current density decreased the efficiency of degradation acceleration. An acceleration factor (AF) was proposed based on the comparison between the number of ions in the mortar under electric field and immersion. Findings from this study are beneficial to develop a reliable acceleration method for the long-term performance of RC structures under chloride and sulfate attack.*

Keywords: *Electric field; Chloride and sulfate attack; Ion content; Degradation; Acceleration factor*

1 Introduction

Chloride ions (Cl-) and sulfate ions (SO_4^{2-}) coexist in salt lakes, saline soils, marine and coastal environments. The degradation process of reinforced concrete (RC) structures under these exposures would be more complex compared to the single chloride or sulfate exposure.

Numerous studies have been conducted on the ionic diffusion and reaction behavior in the cement-based materials under combined chloride and sulfate attack. Cl- was reported to alleviate the damage process of concrete caused by sulfate attack (Du et al. 2019), such as expansion, strength reduction. As the diffusion rate of Cl- is generally 10-100 times higher than that of SO_4^{2-}, cement hydration products firstly react with Cl- to form Friedel's salt, which fills up the pores and blocks the sulfate ingress. The effect of SO_4^{2-} on chloride ingress is still open for discussion. The presence of SO_4^{2-} decreased the chloride penetration fronts and diffusivities of ordinary Portland cement concrete for 60 months (Tumidajski and Chan 1996). However, others reported that the effect of sulfate on chloride diffusion was time-dependent (Metalssi et al. 2023). Although the performance of RC members under combined attack has attracted attention, full immersion or drying-wetting cycle may be insufficient for large-sized RC members. The long-term degradation period limited related researches. Although the performance of RC members under combined attack has attracted attention, full immersion or drying-wetting cycle may be insufficient for large-sized RC members. The long-term degradation period limited related researches.

The electric field has been widely applied to accelerate the chloride ingress into concrete, as well as rebar corrosion. In addition, the electric field was used to speed up sulfate attack. The mineralogical alteration and migration behavior of ionic species in cement-based materials under electric field with sulfate attack was analyzed (Li et al. 2020). Since the electric field has been adopted to accelerate chloride-induced corrosion or sulfate attack, it is of great potential to speed up the degradation of RC members under combined chloride-sulfate attack. Wang et al. (2022) employed an electric field of 30 V to stimulate the sulfate and chloride attack to reinforced concrete, but they focused on the corrosion-induced cracking under different sulfate and chloride environment; the effect of the electric field on the degradation process was not discussed in depth.

This study aims to improve the understanding of the degradation mechanism behind the reinforced concrete under sulfate-chloride exposure and electric field. The steel-mortar samples were exposed to 5% Na_2SO_4, 5% NaCl + 5% Na_2SO_4 solutions and deionized water under two regimes (full immersion, electric field). The efficiency of current density was analyzed. The sulfate content in the mortar under different exposure conditions were analysed. On this basis, an acceleration factor was proposed to assess the acceleration effect of the electric field quantitatively. The microstructural characterization of deteriorated mortar was analyzed by scanning electron microscopy (SEM), energy dispersive X-ray spectroscopy (EDS).

2 Experimental

2.1 Samples Preparation

The Ordinary Portland Cement (P.O 42.5) was used in this study. The natural river sand with a fineness modulus of 2.70 was used as fine aggregate. The mortar mixture was prepared with the water/cement ratio of 0.6 and cement/sand ratio of 1:3. The hot rolled steel plain bars (HPB300) were used. The bars were 10 mm in diameter and 130 mm in length. Cylindrical reinforced mortar samples, 50 mm in diameter and 100 mm high, were prepared. The steel bar was placed in the center. After curing, the top and bottom surfaces of reinforced mortar samples were coated with epoxy resin for one-dimensional uniform transport.

The samples were exposed to solutions with and without electric field, respectively, as shown in Fig. 1. The set-up of the electric field was inspired by the impressed current technique. The steel bar was connected to the positive pole of the power supply and became an anode. The counter electrode, a 304 stainless steel mesh placed around the cylindrical mortar, was connected to the negative pole.

Three different solutions, 5% Na_2SO_4 (S), 5% NaCl + 5% Na_2SO_4 (CS), and deionized water (Q), were prepared. The current density of 0.1 mA/cm^2 was adopted in this study to induce 'natural' corrosion. Another two current densities of 0.2 and 0.5 mA/cm^2, representing the medium (M) and high (H) electric field, were adopted to. Table 1 summarizes the detailed experimental scheme.

2.2 Test Method

2.2.1 *Total and free sulfate ion content*

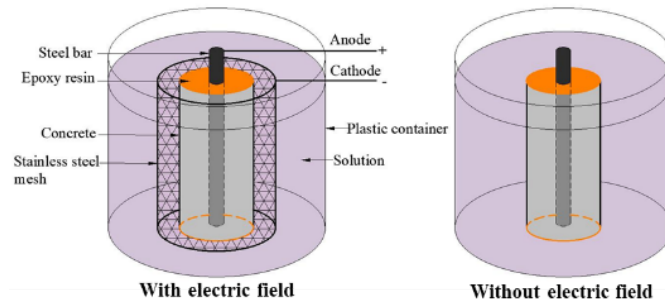The water-soluble and acid-soluble methods were used to determine the total and free SO_4^{2-}

Figure 1. Set-up of exposure conditions

Table 1. Exposure scheme of electric field and immersion.

Group	Exposure regime		Exposure solution	Exposure time / d
S	Electric field	0.1 mA/cm^2	5% Na$_2$SO$_4$	0, 4, 8, 12, 16, 20
CS			5% NaCl + 5% Na$_2$SO$_4$	
Q			Deionized water	
CSM		0.2 mA/cm^2	5% NaCl + 5% Na$_2$SO$_4$	0, 2, 4, 6, 8, 10
CSH		0.5 mA/cm^2	5% NaCl + 5% Na$_2$SO$_4$	0, 0.8, 1.6, 2.4, 3.2, 4
Si	Immersion		5% Na$_2$SO$_4$	0, 60, 120, 180, 240, 300
Csi			5% NaCl + 5% Na$_2$SO$_4$	

contents in the mortar. The powder samples were drilled every 5 mm, then passed a 0.075 mm sieve, and later dried in an oven at 60°C for 24 h. The ultraviolet and visible spectrophotometry (UVPC) method was used to determine SO_4^{2-} content. UV 755B spectrophotometer was used.

2.2.2 *Microstructural analysis*

The microstructure and elemental analysis of the degraded mortar were performed by FEI Quanta 650 FEG environmental SEM equipped with EDS detector. The mortar portions of about 5 mm $\times$ 5 mm were cut by a diamond wire cutting machine at the depths of 2-5 mm (outer layer) and 15-18 mm (inner layer) from the exposed surface, then dried in an oven at 60°C for 24 h. The samples were impregnated with epoxy resin, polished using sandpapers, and carbon-coated. Backscattered electron (BSE) mode were conducted in this study. The accelerating voltage was set to be 20 kV.

3 Results and Discussions

3.1 Sulfate Ion Transport and Reaction Behavior

Figure 2 illustrates the SO_4^{2-} transport and reacted contents under immersion and the electric field of 0.1 mA/cm^2. The reacted SO_4^{2-} content was determined as the difference between total SO_4^{2-} and free SO_4^{2-} measured. In Fig. 2 (a), there was no noticeable difference in the sulfate transport behavior between the two exposure regimes. The content was relatively high near the surface, decreased with the depth, and increased with exposure time. Compared with the diffusion under immersion condition, one could immediately see the acceleration of electric

field on the sulfate transport. The amount of total SO_4^{2-} in the mortar under full immersion for 60 d could be obtained by applying the external electric field of 0.1 mA/cm^2 for 4 d. Moreover, the electric field increased the kinetics of the sulfate reaction, which agreed with previously published work (Lorente et al. 2011). At a depth of 0-5 mm in the mortar, the reacted SO_4^{2-} content is 1.39% after the electric field of 20 d, close to 1.41% after immersion of 300 d.
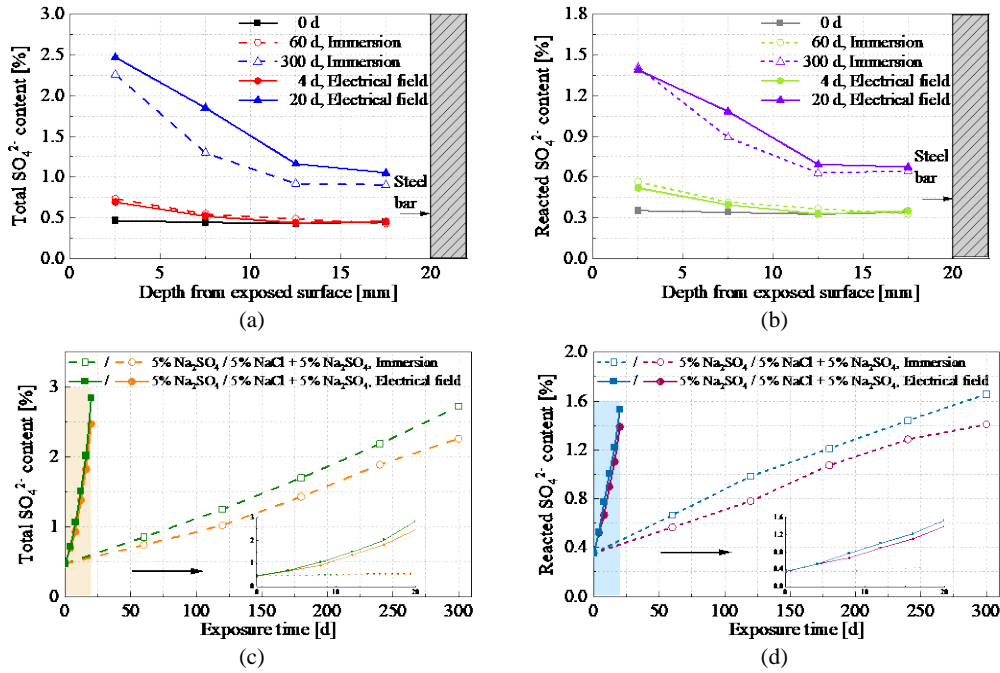

Figure 2. Sulfate content in the mortar under immersion and electric field: (a) total and (b) reacted content profiles in composite solution; (c) total and (d) reacted content in the surface layer of mortar.

Figure 2 (c) and (d) depict the comparison of total and reacted sulfate content in the surface layer (0-5 mm) of mortar between immersion exposure and electric field. It can be seen that the presence of Cl$^-$ retarded sulfate transport and reaction under both exposure conditions. What is interesting is that the inhibitory effect of Cl$^-$ on the SO_4^{2-} transport and reaction attenuated under the electric field. There was a reduction of 13% in the reacted SO_4^{2-} content near the mortar surface after 300 d when the solution changed from the single sulfate solution to the composite solution. The corresponding reduction was 9% under the electric field of 0.1 mA/cm^2 for 20 d. Two reasons could explain this. One was the significant driving force provided by the electric field, and the other was the increased porosity induced by the decomposition of hydration products. Both weakened Friedel's salt clogging the pores and allowed more SO_4^{2-} ingress to the mortar and reacted with hydration products.

3.2 Effect of the Current Density on the Sulfate Reaction

Considering that the sulfate reaction products (ettringite, gypsum) deteriorate mortar, the effect of current density on the reacted SO_4^{2-} content is discussed here. The amount of electric charge during the power-on period is calculated by Eq. (1).

$$Q = iAt \tag{1}$$

where Q is the total amount of electric charge (C); i is the impressed current density (A/cm^2); A is the steel surface where current goes through (cm^2); t is the power-on time (s).

Figure 3 presents the reacted SO_4^{2-} contents at 0-5 mm depth from the exposed surface of mortar exposed to composite solution under the electric field of 0.1, 0.2 and 0.5 mA/cm^2. It can be observed that reacted contents grew as the increase of impressed electric charge. However, the higher the current density, the lower the increase rate of sulfate content. The react SO_4^{2-} content with 0.1 mA/cm^2 reached 1.39%, higher than that of 0.95% with 0.5 mA/cm^2 after the electric charge of 5157 C being applied. Under a higher current density, there is a greater possibility for water molecule splitting, ohmic losses and other reactions to decompose the current (Feng et al. 2021).
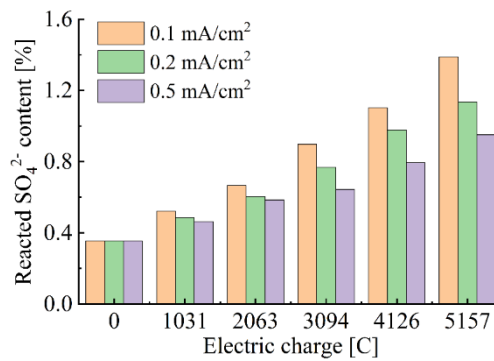

Figure 3. Reacted sulfate contents in the mortar in composite solution under different current densities.

In addition, the effect of current density on the sulfate reaction became more significant in the late stage than early stage. The reacted SO_4^{2-} increased by 0.17%, 0.13%, and 0.11% under 0.1, 0.2, 0.5 mA/cm^2 during the first 1031 C (0-1031 C), while the increases grew to 0.23%, 0.21%, 0.15% during the late 1031 C (3094-4126 C). In the early stage, Friedel's salt and sulfate reaction products filled the pores and clogged the ion migration by the electric field. As the sulfate reaction continued, sulfate reaction products exceeded the pore accommodation and caused microcracks, providing more channels for ions ingress. Thus, the effect of current density manifested in the late stage.

3.3 Acceleration Factor of Electric Field on the Degradation of Reinforced Mortar

To explore an efficient and reliable accelerated method for reinforced concrete under chloride and sulfate attack, an acceleration factor (AF) of the electric field on the degradation process of reinforced mortar was proposed. The reacted SO_4^{2-} were used as degradation indexes since it is the leading cause of mortar deterioration.

The AF was defined as the ratio of the exposure time taken by full immersion to that by the electric field to reach the same number of ions in the mortar. Given that the ion content changes linearly within a specific depth range (from d_i to d_{i+1}, $i=1, 2, 3, 4$). The number of the ions could be determined as the summation of the ions contained in the volume of the mortar portion from d_i to d_{i+1}. The depth range was 5 mm in this study. The initial number of ions should be excluded. Table 2 shows the values of AF under different solutions and current densities. Due to the

relatively low efficiency, the number of ions accumulated under 0.5 mA/cm^2 for 4 d was much smaller than that under immersion for 300 d. Thus, there is a default value in the blank.

Table 2. AF of electric field on the sulfate attack to the mortar.

Full immersion	Exposure time (d)				AF on the sulfate attack			
	Electric field (mA/cm^2)				5% Na$_2$SO$_4$	5% NaCl + 5% Na$_2$SO$_4$		
	5% Na$_2$SO$_4$	5% NaCl + 5% Na$_2$SO$_4$						
	0.1	0.1	0.2	0.5	0.1 mA/cm^2	0.1 mA/cm^2	0.2 mA/cm^2	0.5 mA/cm^2
60	6.0	5.3	3.2	1.5	10.0	11.4	18.7	41.1
120	11.5	9.7	5.6	2.8	10.5	12.4	21.3	43.5
180	14.4	13.4	7.8	3.9	12.5	13.4	23.1	45.7
240	17.3	16.2	9.7	4* (185)	13.9	14.8	24.8	46.3*
300	20* (294)	18.9	10* (249)		14.7*	15.9	24.9*	

*(x) corresponding to the immersion time of x d.

From Table 2, it can be found that AF increased with immersion time at first, the increase slowed down subsequently. AF under composite solution was higher than that under single sulfate solution. It can be explained by the attenuated interaction under electric field. Although AF increased with the current density, higher current density led to less efficiency.

To further investigate the efficiency of electric field on the sulfate deterioration, AFs based on other studies were calculated and listed in Table 3.

Table 3. AF sourced from other studies.

Ref.	Sample	Solution	Electric field regime	Immersion time	SO$_4^{2-}$ content	AF
Lorente et al. 2011	Φ110 mm × 110 mm cylinder.	4% Na$_2$SO$_4$	60 V; 21 d	120 d	Total	27.9
Huang et al. 2016	40 mm cube.	5% Na$_2$SO$_4$	30 V, pulse cycle; 30 d	90 d	Total	11.8
Wang et al. 2022	40 mm cube.	5% Na$_2$SO$_4$	20, 40, 60 V; 90 d	90 d	Total	6, 9, 11
					Reacted	7.2, 10.1, 11.4

In our study, AFs for reacted SO$_4^{2-}$ in 5% Na$_2$SO$_4$ solution were in the range of 10-14.7, close to the range of 11.3-15.8 for total SO$_4^{2-}$. This agreed well with the results in Wang et al.'s study, as shown in Table 3. Thus, both total and reacted SO$_4^{2-}$ content could be used as index of sulfate deterioration. From Table 3, it well proved that the electric field increased the sulfate deterioration on the concrete by several or dozen times. AF was highly dependent on the specimen fabrications and regimes of the electric field. More comparisons between electric field and long-term immersion are required for an efficient and accurate acceleration strategy.

3.4 SEM/EDS Analysis

To further clarify the degradation mechanism behind the electric field, the morphology of the outer layer (near the cathode) and the inner layer (near the anode) were captured in SEM-BSE mode, presented in Fig. 4. The elemental compositions by EDS are shown in Table 3.

Compared Fig. 4 (a) with (b), it can be observed that the microstructure of the outer layer was looser than the inner layer, along with more pores and larger crack widths. This was due to the different reactions between the cathode and anode. Near the cathode, the anions (SO_4^{2-}, Cl^-) quickly migrated into the mortar and reacted with hydration products, resulting in a quick accumulation of reaction products and microcracking. Also, the cation (Ca^{2+}) was forced to leave the mortar, causing the decomposition of portlandite and C-S-H and the increase of porosity. Near the anode, there was a decrease in alkalinity due to the consumption of OH^- in the water electrolysis. This may induce the decomposition of hydration products and microstructural alteration, but the magnitude was smaller than that near the cathode. In addition, the corrosion of the steel bar may partially contribute to the cracks in Fig. 4 (b). In Table 3, Spot A in the outer layer has more content of element S and a lower Ca/Si ratio than Spot B in the inner layer. It well supported the interpretation for morphology alterations above.
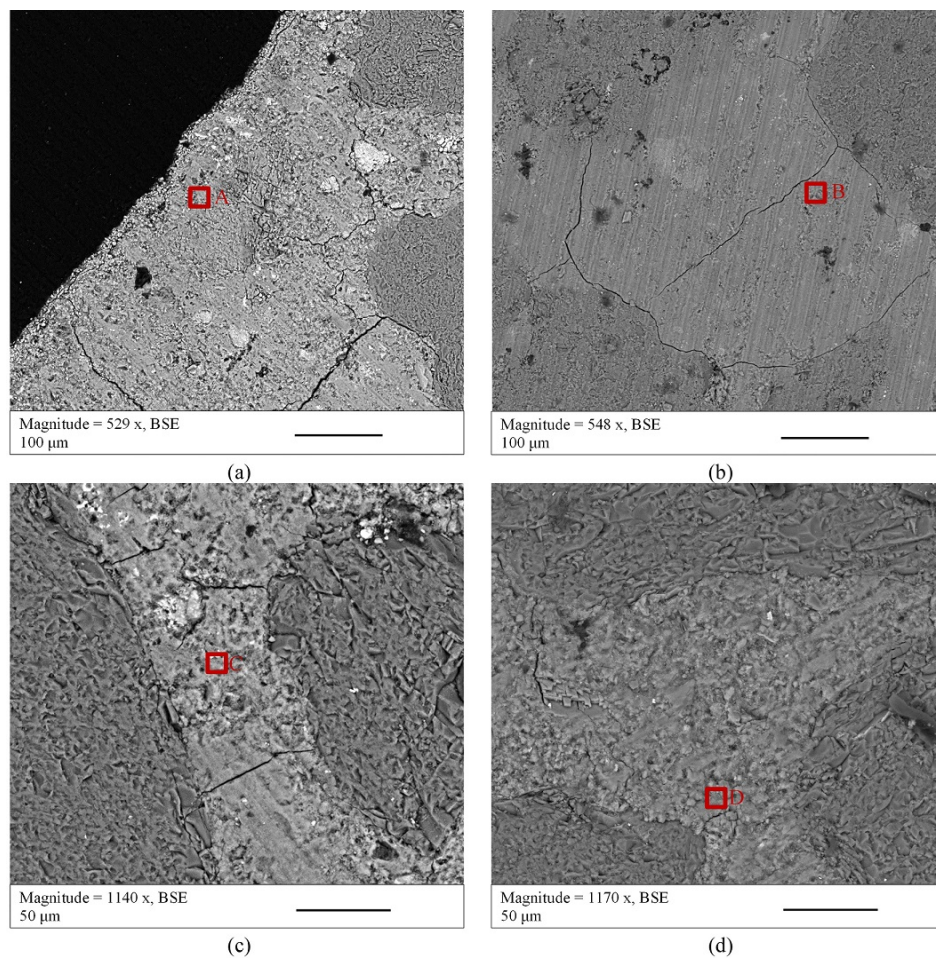

Figure 4. SEM images of different layers in mortar under the electric field. (a) outer layer, composite solution; (b) inner layer, composite solution; (c) outer layer, deionized water; (d) inner layer, deionized water.

7

Table 3. EDS analysis results of spots A, B, C and D.

Spot	C	O	Na	Al	Si	S	Cl	Ca
A	25.93	50.11	0.63	1.21	7.06	2.51	1.3	10.91
B	22.32	51.7	0.27	0.44	7.68	1.34	1.4	13.3
C	34.01	43.61	0.22	2.55	7.86	0.36	0	9.46
D	20.36	62.79	0.46	1.14	4.1	0.32	0	9.99

Figure 4 (c) shows a loose outer microstructure with many pores in the mortar under electric field in deionized water. It was caused by the severe leaching of Ca^{2+} near the cathode, which was confirmed by the low Ca/Si ratio of Spot C in Table 3. Compared to the outer layer, the microstructure of the inner layer looks more compact in Fig. 4 (d), with a higher Ca/Si ratio. In addition, it could be found that the microcracks in the outer and inner layers of the mortar in deionized water were smaller than those in the composite solution. This could be attributed to the absence of aggressive ions and the low corrosion level of the steel bar.

4   Conclusions

- Electric field drastically migrates SO_4^{2-} into the mortar and accelerates sulfate deterioration. The interactions between Cl^- and SO_4^{2-} reduces when the electric field is applied. High current density leads to low efficiency in ion migration.
- In addition to the ion ingress and reaction, the electric field accelerates the decalcification of hydration products. The microstructure near the cathode suffers severe deterioration from sulfate reaction and decalcification.
- AF is proposed based on the comparison between the number of ions accumulated by electric field and full immersion. It well quantifies the acceleration of electric field on the sulfate attack.

The above results are extremely encouraging in the pursuit of degradation acceleration of RC structures. Nevertheless, more studies on the behavior of reinforced concrete under an electric field and combined chloride-sulfate attack are required.

References

Du, J., Tang, Z., Li, G., Yang, H. and Li, L. (2019). *Key inhibitory mechanism of external chloride ions on concrete sulfate attack*. Construction and Building Materials, 225, 611–619.

Feng, W., Dong, Z., Liu, W., Cui, H., Tang, W. and Xing, F. (2021). *An experimental study on the influence of applied voltage on current efficiency of rebars with a modified accelerated corrosion test*. Cement and Concrete Composites, 122, 104120.

Huang, Q., Wang, C., Zeng, Q., Yang, C., Luo, C., Yang, K. (2016). *Deterioration of mortars exposed to sulfate attack under electrical field*. Construction and Building Materials, 117, 121–128.

Li, C., Jiang, Z., Myers, R. J., Chen, Q., Wu, M., Li, J. and Monteiro, P. J. M. (2020). *Understanding the sulfate attack of Portland cement–based materials exposed to applied electric fields: Mineralogical alteration and migration behavior of ionic species*. Cement and Concrete Composites, 111, 103630.

Lorente, S., Yssorche-Cubaynes, M. P. and Auger, J. (2011). *Sulfate transfer through concrete: Migration and diffusion results*. Cement and Concrete Composites, 33(7), 735–741.

Metalssi, O.O., Touhami, R.R., Barberon, F., d'Espinose de Lacaillerie, J.B., Roussel, N. Divet, L. and Torrenti, J.M. (2023). *Understanding the degradation mechanisms of cement-based systems in combined chloride-sulfate attack*. Cement and Concrete Research, 164, 107065

Tumidajski, P.J. and Chan, G.W. (1996). *Effect of sulfate and carbon dioxide on chloride diffusivity*. Cement and

Concrete Composites, 26, 551–556.

Wang, B., Li, G. and Panesar, D.K. (2022). *A study of variables that affect the process of sulfate attack of cement-based materials subjected to stray current*. Structural Concrete, 23, 706–721.

Wang, X., Liu, J., Jin, Z., Chen, F., Zhong, P. and Zhang, L. (2022). *Real-time strain monitoring of reinforced concrete under the attacks of sulphate and chloride ions based on XCT and DIC methods*. Cement and Concrete Composites, 125, 104314.